

# Neutron wave packet tomography

G. Badurek,<sup>1</sup> P. Facchi,<sup>2,3</sup> Y. Hasegawa,<sup>1</sup> Z. Hradil,<sup>4</sup> S. Pascazio,<sup>2,3</sup> H. Rauch,<sup>1</sup> J. Řeháček,<sup>4</sup> and T. Yoneda<sup>2,5</sup>

<sup>1</sup>*Atominstitut der Österreichischen Universitäten, Stadionallee 2, A-1020 Wien, Austria*

<sup>2</sup>*Dipartimento di Fisica, Università di Bari, I-70126 Bari, Italy*

<sup>3</sup>*Istituto Nazionale di Fisica Nucleare, Sezione di Bari, I-70126 Bari, Italy*

<sup>4</sup>*Department of Optics, Palacký University, 17. listopadu 50, 772 00 Olomouc, Czech Republic*

<sup>5</sup>*School of Health Sciences, Kumamoto University, 862-0976 Kumamoto, Japan*

A tomographic technique is introduced in order to determine the quantum state of the center of mass motion of neutrons. An experiment is proposed and numerically analyzed.

In experimental physics one often faces the following question: “Given the outcomes of a particular set of measurements, which quantum state do they imply?” Such *inverse problems* may arise for instance when setting up and calibrating laboratory sources of quantum states, or in the analysis of decoherence and other deteriorating effects of the environment, or in some special tasks in quantum information processing such as eavesdropping on a quantum channel in quantum cryptography.

The determination of the quantum state represents a highly nontrivial problem, whose history can be traced back to the early days of quantum mechanics, namely to the Pauli problem [1, 2]; the experimental validation had to wait until quantum optics opened a new era. The theoretical predictions of Vogel and Risken [3] were closely followed by the experimental realization of the suggested algorithm by Smithey *et al.* [4]. Since then many improvements and new techniques have been proposed: an up-to-date overview can be found in Ref. [5]. Recent progress in instrumentation has made it possible to apply these techniques to a variety of different quantum systems such as fields in optical cavities, polarization and external degrees of freedom of photons, or motional states of atoms.

In this Letter we propose an experiment for determining the quantum states of the center-of-mass motion of neutrons. In accordance with quantum theory, these massive particles can be associated with a wave function describing their motional state. Neutrons are suitable objects for many quantum mechanical experiments due to their interaction with all four basic forces, the ease of detecting them with almost 100% efficiency, and their small coupling to the environment [6]. In marked contrast with light, neutron vacuum field and thermal background can usually be ignored. This makes it possible, for instance, to prepare superpositions of macroscopically separated quantum states—the so-called Schrödinger cat states—that would be extremely difficult to realize with other quantum systems because of their fragility with respect to decoherence. In all experiments performed so far, the existence of the Schrödinger cat states of neutrons has been indirectly demonstrated via interferometric effects, but the full evidence for the nonclassicality of these states, including the presence of the negative values

of the reconstructed Wigner function, is still missing.

In the following, we will first briefly review the present neutron interferometric techniques and the means of creating highly nonclassical motional states of neutrons. In the second part of the Letter, an experiment will be proposed for the complete reconstruction of these quantum states.

**Neutron tomography** - The set of measurements that can be done on neutrons to determine their quantum state is severely limited by the very low time resolution of the available detectors. In quantum optics, this obstacle can be overcome by mixing the weak input field with a strong local oscillator. By changing the phase  $\phi$  of the oscillator one can measure the spectral decompositions of all quadratures,

$$\hat{X}_\phi = \hat{x} \cos \phi + \hat{p} \sin \phi, \quad (1)$$

$\hat{x}$  and  $\hat{p}$  being the canonically conjugated operators of position and momentum. Of course, no such local oscillators exist for neutrons. However, notice that massive particles experience a transformation of the type (1) in the course of free evolution:  $x(t) = x + (p/m)t$ , where  $m$  is the mass. Thus free evolution of the wave packet followed by a position sensitive measurement yields information about a subset of quadratures  $X_\phi$ ,  $\phi \in [0, \pi/2]$ . Free evolution was utilized e.g. for the reconstruction of transversal motional states of helium atoms in [7]. Here we are interested in the *longitudinal* degrees of freedom. Since neutron detectors have very bad time resolution, free evolution *alone* cannot be used to generate a tomographically complete set of measurements.

Feasible measurements on thermal neutrons consist of measurements of the contrast and phase of interference fringes in an interferometric setup, see Fig. 1 (without momentum kick), and also spectral analysis of the neutron beam using an adjustable Bragg-reflecting crystal plate together with a position sensitive detector. This set of observables is *not* tomographically complete because the measurable (complex) contrast of the interference pattern [6] ( $\hbar = 1$ ),

$$\Gamma(\Delta x) = \langle \psi | e^{i\Delta x \hat{p}} | \psi \rangle = \int |a(p)|^2 e^{i\Delta x p} dp, \quad (2)$$

is not sensitive to the phase of  $a(p) = \langle p | \psi \rangle$ , and no information about quadratures other than  $p$  is available.

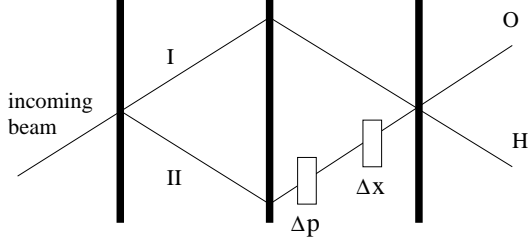


FIG. 1: Scheme of a perfect crystal neutron interferometer. The incoming beam is split at the first crystal plate, reflected at the middle plate and recombined again at the third plate. The detector is placed in beam O where the visibility is higher due to the same number of reflections/transmissions. In addition to a position shift  $\Delta x$  routinely used in neutron experiments, a momentum kick  $\Delta p$  has been added in path II in order to make the interferometric measurement tomographically complete; see text.

Obviously, the situation would be different if one could shift both the position (phase) *and* the momentum of the incoming wave packet inside the interferometer. Such a thought experiment is shown in Fig. 1. In that case, the Wigner function describing the ensemble of measured neutrons would be related to the measured contrast

$$\Gamma(\Delta p, \Delta x) = \text{tr} \{ \rho e^{i\Delta p \hat{x}} e^{i\Delta x \hat{p}} \} = \int e^{i(\Delta p)x} \langle x | \rho | x + \Delta x \rangle dx \quad (3)$$

by a simple integral transformation,

$$W(x, p) = \iint e^{-i\frac{uv}{2} + iux + ivp} \Gamma(-u, v) du dv, \quad (4)$$

where  $u = \Delta p$ ,  $v = \Delta x$  and  $\rho$  is the state to be reconstructed.

Although this thought experiment looks simple, its experimental realization, according to Fig. 1, would be rather difficult. Large momentum kicks acquired by the neutron in the lower arm would change its de Broglie wavelength and spoil the Bragg reflection at the last crystal plate. Therefore we will now propose a modified scheme that can substitute the interferometric setup of Fig. 1.

**Setup** - In the new scheme shown in Fig. 2, the incoming neutrons polarized in the  $+z$  direction,  $|\Psi\rangle = |\psi\rangle|z_+\rangle$ , where  $\psi$  denotes the spatial degrees of freedom, first propagate freely through a distance  $L$ , undergoing a unitary operation  $U_1 = \exp[-i\hat{p}^2 L/(2p_0)]$ . In the following, we will assume that the input wave packets are quasi-monochromatic,  $\sigma_p/p_0 \simeq$  a few percent, with spread  $\sigma_p$  and central momentum  $p_0$ . This condition guarantees that the action of the RF coil is practically equivalent to a momentum “kick.” The generalization to more general states will be presented elsewhere. After the region of free propagation, the neutrons are let through an RF coil placed in a static magnetic field polarized along the

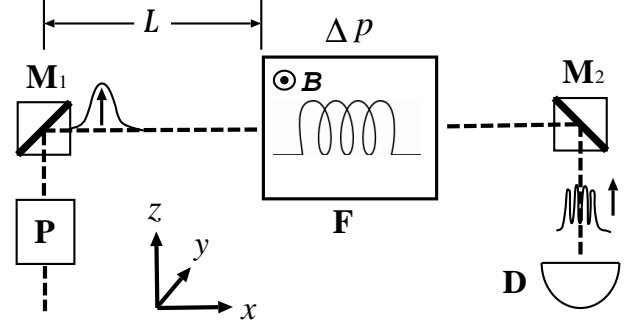


FIG. 2: Setup for the tomography of motional states of neutrons.  $M_1, M_2$  – magnetic mirrors;  $L$  – region of free propagation;  $B$  – static magnetic field controlling the momentum kick  $\Delta p$ ;  $F$  – box containing a static magnetic field (aligned along  $+y$ ) and an RF coil;  $D$  – detector; the state is “prepared” by  $P$ , which can be a chopper or a monochromator. The arrows denote the polarization of neutrons after reflections from magnetic mirrors.

$-y$  direction, see Fig. 2. As a result of the interaction between the neutron and the coil, the  $y_+$  ( $y_-$ ) component of the input state will be decelerated (accelerated). Assuming that the region of interaction is short, so that the dispersion of the wave packet of the neutron can be neglected in the coil, in the quasi-monochromatic approximation, the net momentum transfer can be described by the effective unitary operator,

$$U_2 = e^{-i\Delta p \hat{x}/2} |y_-\rangle \langle y_+| + e^{i\Delta p \hat{x}/2} |y_+\rangle \langle y_-|, \quad (5)$$

where

$$\Delta p = \frac{2\mu B m}{p_0}. \quad (6)$$

Prior to detection, the particles are polarized along the  $+z$  direction again, so as to erase the which-way information stored in the polarization degree of freedom. The probability of a neutron being detected is given by the norm of the transmitted component,

$$P = \text{Tr}\{\Pi(\Delta p, \Delta x)\rho\}, \quad (7)$$

where  $\rho$  refers only to the spatial degrees of freedom and

$$\begin{aligned} \Pi(\Delta p, \Delta x) &= \langle z_+ | U_1^\dagger U_2^\dagger | z_+ \rangle \langle z_+ | U_2 U_1 | z_+ \rangle \\ &= (1 + e^{i\frac{L}{2p_0} \hat{p}^2} e^{i\Delta p \hat{x}} e^{-i\frac{L}{2p_0} \hat{p}^2})/4 + \text{h.c.} \\ &= (1 + e^{i\Delta p(\hat{x} + L\hat{p}/p_0)})/4 + \text{h.c.} \\ &= (1 + e^{i\Delta x \hat{p}} e^{i\Delta p \hat{x}} e^{-i\Delta x \Delta p/2})/4 + \text{h.c.}, \end{aligned} \quad (8) \quad (9) \quad (10)$$

where we denoted

$$\Delta x = \frac{\Delta p L}{p_0} = \frac{2\mu B m L}{p_0^2}. \quad (11)$$

Direct inversion - The detection probability (7) reads

$$P(\Delta p, \Delta x) = \frac{1}{2} + \frac{1}{2} \text{Re}\{\Gamma(\Delta p, \Delta x) e^{2i\Delta x \Delta p}\}. \quad (12)$$

Since the beam is quasi-monochromatic one has for  $\delta x = \pi/2p_0$ ,

$$\Gamma(\Delta p, \Delta x + \delta x) \simeq \Gamma(\Delta p, \Delta x) e^{i\pi/2} \quad (13)$$

from which the imaginary part of the complex degree of coherence  $\Gamma(\Delta p, \Delta x)$  can be obtained.

Summarizing, the tomography of a neutron state consists in the following four steps:

(i) A set of pairs of independent variables  $\{B_j, L_j\}$  is chosen covering a certain range  $B \in [0, B_{\max}]$  and  $L \in [0, L_{\max}]$ .

(ii) For each pair  $B_j, L_j$  the shifts  $\Delta p_j$  in (6) and  $\Delta x_j$  in (11) are calculated, and the corresponding intensities  $P(\Delta p_j, \Delta x_j)$  are measured with and without an auxiliary shift  $\delta x = \pi/2$ .

(iii) The complex degree of coherence  $\Gamma(\Delta p_j, \Delta x_j)$  is calculated from the two intensities using Eqs. (12)-(13).

(iv) Finally, the Wigner function of the input neutrons is calculated with the help of inversion formula (4), where the integrals are approximated by sums over  $\Delta x_j$  and  $\Delta p_j$ .

According to (4), the contrast  $\Gamma(\Delta p, \Delta x)$  is essentially the Fourier transform of the Wigner function  $W(x, p)$ . Therefore the largest values of  $\Delta p$  and  $\Delta x$  are related to the smallest resolved details in  $x$  and  $p$  respectively. Namely (reinserting  $\hbar$ ),

$$\Delta p_{\text{MAX}} = \hbar/\delta x_{\min}, \quad \Delta x_{\text{MAX}} = \hbar/\delta p_{\min}, \quad (14)$$

where  $\delta x_{\min}$  and  $\delta p_{\min}$  denote the  $x$  and  $p$  resolutions. By (6) and (11) one gets

$$\delta x_{\min} = \frac{\hbar}{2\mu m} \frac{p_0}{B_{\text{MAX}}}, \quad \delta p_{\min} = \frac{p_0}{L} \delta x_{\min}. \quad (15)$$

For a neutron of wavelength  $\lambda_0 = 0.37\text{nm}$  [8], assuming the reasonable values  $L_{\text{MAX}} = 1\text{m}$  and  $B_{\text{MAX}} = 0.1\text{T}$  one gets  $\delta x_{\min} = 60\mu\text{m}$  and  $\delta p_{\min} = \hbar \times 10^6\text{m}^{-1}$ .

Radon inversion - It is interesting to give an alternative interpretation of the proposed measurement in Fig. 2. Notice, that the POVM elements in Eq. (9) can also be restated in terms of quadrature operators,

$$\Pi(\Delta p, \Delta x) = (1/4)(1 + e^{i\omega \hat{X}_\theta}) + \text{h.c.}, \quad (16)$$

where (in fixed units)

$$\hat{X}_\theta = \cos \theta \hat{x} + \sin \theta \hat{p}, \quad \tan \theta = \frac{\Delta x}{\Delta p} = \frac{L}{p_0}, \quad (17)$$

and  $\omega = \sqrt{\Delta x^2 + \Delta p^2}$ . Thus, for a fixed  $\theta$ , the data contain information about the characteristic function of

the quadrature  $\hat{X}_\theta$ ,

$$P(\Delta p, \Delta x) = 1/2 + \text{Re}\{C_{X_\theta}(\omega)\}/2, \quad (18)$$

$$\langle C_{X_\theta}(\omega) \rangle = \int P_{X_\theta}(x) e^{i\omega x} dx. \quad (19)$$

By changing  $L$  one changes the quadrature measured, while  $\omega$ , which depends on both  $L$  and  $B$ , determines the observed spatial frequency of the probability distribution of this quadrature. The observed quadratures range from  $\hat{x}$  (for  $L = 0$ ) to  $\hat{p}$  (for  $L \rightarrow \infty$ ). From the measurement of  $C_{X_\theta}(\omega)$ , the “shadows”  $P_{X_\theta}(x)$  of the Wigner function can be obtained by the Fourier transformation, which in turn yield the Wigner function by an inverse Radon transformation. This is an alternative way of reconstruction the Wigner function from the measured data in the setup Fig. 2.

Statistical inversion - The procedures outlined above, based on the direct inversion formula (4), have several drawbacks: (i) Realistic data are always noisy. In that case, formula (4) can yield unphysical results, such as the Wigner representation of a non-positive definite operator. (ii) The Wigner function in Eq. (4) depends on the measured data indirectly, through the complex degree of coherence  $\Gamma$ , which itself has to be estimated with the help of an auxiliary position shifter. This intermediate step is, certainly, not necessary as all available information about the Wigner function of the incoming neutrons is contained in the raw data measured without any auxiliary position shift. In order to avoid these problems, we propose to use the maximum-likelihood quantum state reconstruction [5, 9, 10]. The main advantages of this method compared to the above direct inversion are: (i) Asymptotically, for large data samples it provides the best performance available. (ii) Any prior information about the measured neutrons and the known statistics of the experiment can be used to increase the accuracy of the reconstruction. (iii) The existing physical constraints can be easily incorporated into the reconstruction. Most notably, this technique guarantees the positivity of the reconstructed density operator. (iv) It can be applied directly to raw counted data.

Assuming that the statistics of the experiment is Poissonian, the maximum-likelihood reconstruction amounts to minimizing the Kullback-Leibler distance (relative entropy) between the measured data  $f(\Delta x, \Delta p)$  and the renormalized theoretical probabilities  $p(\Delta x, \Delta p)/\sum p$  of Eq. (12). As has been shown in [9, 10], the maximum-likely density matrix can be obtained as a fixed point of the iterations of a nonlinear operator map.

As follows from the parameter estimates given after Eq. (15), the proposed tomography scheme using thermal neutrons will likely have sufficient resolution in momentum. On the other hand, even for well monochromatized thermal beams, the resolution in position is expected to be worse (possibly even by several orders of

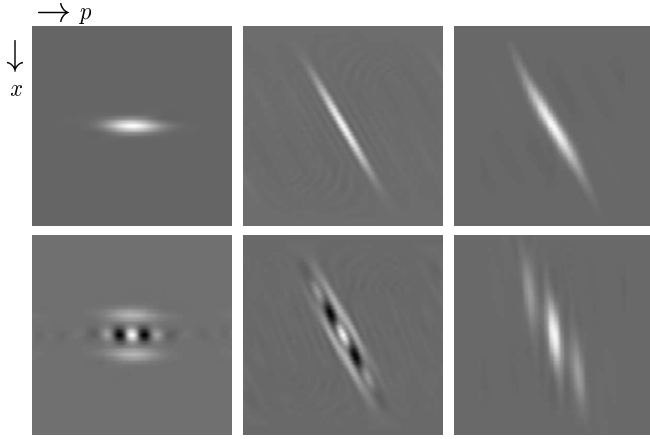


FIG. 3: Reconstructed Wigner functions of Gaussian states (upper row) and superpositions of Gaussian states (“cats;” lower row) from the simulated data. A  $50 \times 50$  matrix of  $\Delta x$  and  $\Delta p$  shifts was used for the maximum-likelihood inversion. Left column: reconstructed original states; middle column: reconstructed time-evolved states with a resolution  $\delta x_{\min}/l_{\text{coh}} = 1/2$ ; right column: reconstructed time-evolved states with reduced resolution,  $\delta x_{\min}/l_{\text{coh}} = 10$ . Grey is the zero level, white (black) represents positive (negative) values.

magnitude) than typical coherence lengths. The simulations in Figure 3 illustrate the effect of the restricted range of  $\Delta p$  on the reconstruction. Consider first the reconstruction of a minimum uncertainty Gaussian wave packet in its moving frame, parameterized by its coherence length  $l_{\text{coh}}$ ,  $|\Psi_G\rangle \propto \int \exp(-k^2 l_{\text{coh}}^2/2) |k\rangle dk$ . (The choice of a minimum uncertainty state is only for illustrative purposes.) Provided the apparatus has a sufficient spatial resolution,  $\delta x_{\min} < l_{\text{coh}}$ , a faithful reconstruction is readily obtained, see the upper left panel. More realistic measurement with  $\delta x_{\min} > l_{\text{coh}}$  would obviously yield a Wigner function smoothed out along the  $x$  axis. However, the states measured in a real experiment are not going to be minimum uncertainty states. The experimenter will rather deal with time evolved states  $|\Psi(T)\rangle \propto \int \exp(ik^2 T/2m - k^2 l_{\text{coh}}^2/2) |k\rangle dk$  that are strongly affected by dispersion. As a consequence, the wave packet spread very soon becomes larger than the resolution limit,  $\delta x_T \sim T/(ml_{\text{coh}}) \gg \delta x_{\min}$ , and a good reconstruction can be achieved with a realistic apparatus. Compare the upper middle and right panels, showing reconstructions with a sufficient resolution  $\delta x_{\min} = l_{\text{coh}}/2$  and a reduced (but more realistic) resolution  $\delta x_{\min} = 10l_{\text{coh}}$ .

The imaging of non-classical states is a much more delicate problem. Let us consider the superpositions of spatially separated Gaussian states (Schrödinger cats),  $|\Psi_{\text{cat}}\rangle \propto [1 + \exp(i\hat{p}\Delta)]|\Psi_G\rangle$ . Such states can be prepared e.g. by means of a double loop perfect crystal interferometer [11]. As has been shown [8], the preparation of thermal neutron cat states is possible, with separations exceeding the corresponding coherence lengths of the in-

dividual components  $\Delta \gg l_{\text{coh}}$ . Provided the apparatus has sufficient resolution, the nonclassicality of this state is manifested by the negative regions of the reconstructed Wigner function, see the lower left panel of Fig. 3. Taking dispersion into account, the ordering of the relevant parameters is  $l_{\text{coh}} < \Delta < \delta x_T$ , and one can easily obtain  $\delta x_{\min} < \delta x_T$ . As the simulations show, a realistic measurement whose position resolution is much worse than the coherence lengths of the individual cat state components tends to wipe out the negative regions of the reconstructed Wigner function; compare the lower middle and right panels of Fig. 3. On the other hand, the main features of such exotic states, such as their non-Gaussian character and also the global spatial properties of which little is known today, should still be accessible to a realistic wave packet tomography. To resolve more subtle quantum interference effects of the order of the coherence length, more refined experimental techniques may however be needed. An idea could be to replace thermal neutrons by ultracold neutrons, for which much larger momentum shifts  $\Delta p$  (and thus much smaller  $\delta x_{\min}$ , possibly even smaller than  $\Delta$ ) can be obtained.

In conclusion, we have proposed and analyzed an experimental scheme for determining the motional states of neutrons. With the help of a magnetic field and free propagation, this apparatus realizes quadrature measurements on neutrons by measuring overlaps of the two transformed components of the initial state. This is an analog of the quantum optical homodyne detection in neutron optics, achieved without the use of a strong coherent source of neutrons.

This work was supported by the Bilateral Research Program between Italy and the Czech Republic PH1 on “Decoherence and Quantum Measurements” and by the Research Project MSM 6198959213 of the Czech Ministry of Education.

- 
- [1] S. Weigert, Phys. Rev. A **45**, 7688 (1992).
  - [2] S. Weigert, Phys. Rev. A **53**, 2078 (1996).
  - [3] K. Vogel and H. Risken, Phys. Rev. A **40**, 2847 (1989).
  - [4] D. T. Smithey, M. Beck, M. G. Raymer, and A. Faridani, Phys. Rev. Lett. **70**, 1244 (1993).
  - [5] M. Paris and J. Řeháček, eds., *Quantum State Estimation*, vol. 649 of *Lecture Notes in Physics* (Springer, Berlin, 2004).
  - [6] H. Rauch and S. A. Werner, *Neutron Interferometry* (Oxford University Press, Oxford, 2000).
  - [7] C. Kurtsiefer, T. Pfau, and J. Mlynek, Nature **386**, 150 (1997).
  - [8] G. Badurek, H. Rauch, M. Suda, and H. Weinfurter, Optics Communication **179**, 13 (2000).
  - [9] Z. Hradil, Phys. Rev. A **55**, 1561(R) (1997).
  - [10] J. Řeháček, Z. Hradil, and M. Ježek, Phys. Rev. A **63**, 040303(R) (2001).
  - [11] M. Baron, H. Rauch, and M. Suda, J. Opt. B: Quantum and Semiclass. Opt. **5**, S241 (2003).